

# Adver-City: Open-Source Multi-Modal Dataset for Collaborative Perception Under Adverse Weather Conditions

Mateus Karvat<sup>1</sup> and Sidney Givigi<sup>1</sup>

**Abstract**—Adverse weather conditions pose a significant challenge to the widespread adoption of Autonomous Vehicles (AVs) by impacting sensors like LiDARs and cameras. Even though Collaborative Perception (CP) improves AV perception in difficult conditions, existing CP datasets lack adverse weather conditions. To address this, we introduce Adver-City, the first open-source synthetic CP dataset focused on adverse weather conditions. Simulated in CARLA with OpenCDA, it contains over 24 thousand frames, over 890 thousand annotations, and 110 unique scenarios across six different weather conditions: clear weather, soft rain, heavy rain, fog, foggy heavy rain and, for the first time in a synthetic CP dataset, glare. It has six object categories including pedestrians and cyclists, and uses data from vehicles and roadside units featuring LiDARs, RGB and semantic segmentation cameras, GNSS, and IMUs. Its scenarios, based on real crash reports, depict the most relevant road configurations for adverse weather and poor visibility conditions, varying in object density, with both dense and sparse scenes, allowing for novel testing conditions of CP models. Benchmarks run on the dataset show that weather conditions created challenging conditions for perception models, reducing multi-modal object detection performance by up to 19%, while object density affected LiDAR-based detection by up to 29%. The dataset, code and documentation are available at <https://labs.cs.queensu.ca/quarrg/datasets/adver-city/>.

## I. INTRODUCTION

Self-driving cars are here, with robotaxi companies in the USA and China having already logged over 60 million fully autonomous miles [1]. However, Autonomous Vehicles (AVs) still have a long road ahead before reaching widespread adoption. Many issues must still be addressed to ensure AVs can drive safely and reliably in all possible scenarios.

Adverse weather conditions such as rain, fog, and glare present significant challenges for AVs. Although these conditions do not constitute the most common driving conditions, they create particularly difficult driving scenarios. For instance, it only rains over land 8% of the time [2] but the risk of accidents in rainy weather is 70% higher than normal [3]. Additionally, these conditions degrade the performance of perception sensors like cameras and LiDARs [4].

A promising solution to this challenge is Collaborative Perception (CP) [5], a growing field within self-driving research. In CP, Connected AVs (CAVs) share information about their surroundings with each other, an approach called V2V (Vehicle-to-Vehicle) collaboration, or also with other entities such as Roadside Units (RSUs), an approach called V2X (Vehicle-to-Everything) collaboration. CP significantly

enhances a vehicle’s perception capabilities [6], especially in situations involving occlusion or long-range detection [7], and is expected to offer similar benefits in adverse weather conditions.

However, the field faces a shortage of adverse weather datasets, as there is currently no open-source CP dataset focused on such conditions. Existing open-source datasets have no adverse weather scenes, while the ones that have adverse conditions offer little weather diversity and are not open-source, preventing scene modifications to expand weather variety.

We introduce Adver-City, the first open-source CP dataset focused on adverse weather conditions, created using the CARLA simulator [8] and OpenCDA framework [9]. The dataset includes 110 diverse scenarios across six distinct weather conditions: clear weather, glare, soft rain, heavy rain, fog and foggy heavy rain (Fig. 1). It is the first synthetic CP dataset to feature glare and incorporate real-life data on adverse weather and poor visibility conditions in its scenario design. Each scene includes three CAVs and two RSUs, and multi-modal data from LiDARs, RGB and semantic cameras, GNSS, and IMUs, supporting tasks like object detection and tracking, as well as semantic segmentation.

Our key contributions could then be summarized as:

- Adver-City, the first open-source synthetic CP dataset focused on adverse weather conditions;
- Glare scenarios, which have not yet been explored by CP datasets;
- A scenario design approach based on real-life data that accounts for challenging conditions involving adverse weather and poor visibility;
- A sensor suite balancing performance and real-world feasibility, supported by sensor configurations commonly used in practice and enabling Sim2Real approaches.

This paper is organized as follows: Section II presents and discusses synthetic multi-modal CP datasets, Section III describes the Adver-City dataset in regards to its scenarios, generation and statistics, Section IV presents the results of benchmarks performed with the dataset, and Section V discusses possible directions to be taken in the future.

## II. RELATED WORK

Collaborative Perception has gained considerable attention recently, leading to the development of various datasets. Some, like DAIR-V2X [10], V2V4Real [11] and TUM-Traf [12], are based on real-world data, while others use synthetic data from simulators such as CARLA [8] and

<sup>1</sup>School of Computing, Queen’s University, Kingston, ON, Canada  
 {mateus.karvat, sidney.givigi}@queensu.ca

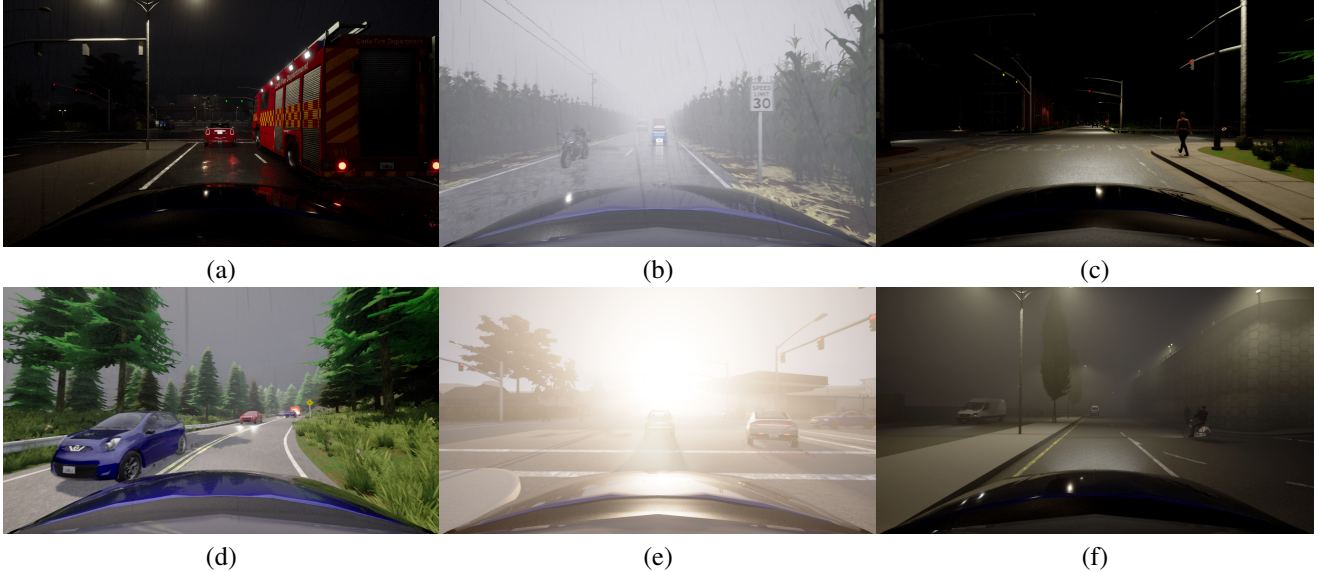


Fig. 1: Camera samples from Adver-City showcasing its weather diversity. (a) Heavy rain night at an urban intersection. (b) Foggy heavy rain day at a rural straight non-junction. (c) Clear night at a rural intersection. (d) Soft rain day at a rural curved non-junction. (e) Glare day at an urban intersection. (f) Foggy night at an urban non-junction.

LidarSIM [13]. Among the synthetic datasets, some focus solely on LiDAR data, such as V2V-Sim [14] and CODD [15], while others provide multi-modal data from both LiDARs and cameras, as shown in Table I and discussed here.

OPV2V [16] is arguably the most used CP dataset, serving as a benchmark for several collaborative models, including Coalign [20], Where2Comm [21] and CoBEVT [22]. Built with the open-source OpenCDA framework [9], it has inspired variations such as OPV2V-H [23], OPV2V+ [24] and OPV2VH+ [25]. However, it does not contain RSUs, includes only one object category (cars), and features only clear weather scenarios.

Another widely used dataset is V2X-Sim [17], which was used in models such as STAR [26], SyncNet [27] and DiscoNet [28]. It follows the annotation schema of the single-vehicle NuScenes dataset [29], featuring RSUs, semantic segmentation ground truths, and multiple object categories. However, it lacks adverse weather scenes and does not provide the source code for scenario generation, limiting its modifiability.

The DOLPHINS [18] dataset, while open-source, is less commonly used and built on a less robust codebase than OpenCDA’s [9]. Additionally, it includes only six clear weather scenarios with data captured from a LiDAR sensor and a single front-facing camera per agent.

Focusing on accident prediction, DeepAccident [7] features a large number of scenarios with diverse object categories, including pedestrians and two-wheeled vehicles. The scenes, selected based on real-world crash reports, include a few environmental conditions – 37% are rainy, and 16.3% occur at night. However, the scenario generation code is not publicly available, and, due to its focus on accident

prediction, the scenes are short, averaging less than 9 seconds in length.

The recent SCOPE dataset [19] performs image and point cloud augmentation on top of CARLA’s sensor data to provide more realistic weather. It includes data from digital twin maps of German cities and a solid-state LiDAR among its sensors. Despite its focus on adverse weather, only 44.2% of its scenes feature fog or rain, and just 25.8% take place at night. Additionally, the scenario generation code has not been made publicly available.

### III. ADVER-CITY DATASET

#### A. Scenarios

Inspired by DeepAccident [7], we selected scenarios based on comprehensive real-world crash data from the US National Highway Traffic Safety Administration (NHTSA). Even though accidents involving AVs are fundamentally different from those involving only non-autonomous vehicles (over 90% of crashes are caused by driver error [30]), data on AV crashes remains scarce. Public AV crash reports document only 30 [31] or fewer [32] AV crashes, compared to the latest NHTSA report [33], which records over 5 million accidents for non-autonomous vehicles.

An NHTSA report from 2007 [34] defined a typology consisting of 37 pre-crash scenarios based on vehicle movements and the critical event occurring immediately before a crash, presenting detailed statistics on each scenario. However, in 2019, another NHTSA report [33] updated the typology to a total of 36 pre-crash scenarios, clustering them in 9 scenario groups (Table II) and providing up-to-date statistics on each group.

Since the main problems for object detection under adverse weather conditions may be attributed to poor visibility

Dataset	V2X	View-points	Scenes	Frames (k)	Annotations (k)	Categories	RGB	Lidar	Semantic	GNSS & IMU	Weather	Open Source
OPV2V [16]	V2V	2-7	73	11	233	1	✓	✓	✗	✓	✗	✓
V2X-Sim [17]	V2X	2-7	100	10	-	23	✓	✓	✓	✓	✗	✗
DOLPHINS [18]	V2X	3	6	42	293	2	✓	✓	✗	✗	✗	✓
DeepAccident [7]	V2X	5	691	57	-	6	✓	✓	✓	✓	✓	✗
SCOPE [19]	V2X	3-24	44	17	575	5	✓	✓	✓	✗	✓	✗
Adver-City	V2X	5	110	24	889	6	✓	✓	✓	✓	✓	✓

TABLE I: Comparison between multi-modal CP datasets generated using CARLA [8]. The number of annotations for V2X-Sim and DeepAccident is not provided by their authors. All datasets are publicly available, yet only the Open Source datasets provide scenario generation code.

Scenario Group	Weather*	Bad Visibility*	Fatality Rate (%)	Vehicles per Crash <sup>†</sup>
Animal	10	1	0.03	1.02
Rear-End	12	1	0.07	<b>2.19</b>
Lane Change	10	2	0.12	2.00
Crossing Paths	11	<b>7</b>	0.35	<b>2.04</b>
Control Loss	<b>44</b>	1	0.95	1.16
Pedalcyclist	5	<b>7</b>	1.08	1.05
Road Departure	13	2	1.19	1.01
Opposite Direction	<b>15</b>	4	<b>3.23</b>	1.88
Pedestrian	13	<b>10</b>	<b>5.29</b>	1.07

TABLE II: Statistics from the latest NHTSA report [33] on pre-crash scenario groups. The highest two values in each column are highlighted for convenience. \*Percentage of crashes in each scenario group that had adverse conditions as the main factor. <sup>†</sup>Average number of vehicles per crash in each group.

and sensor performance degradation [35], we filtered the pre-crash scenarios groups by focusing on those that have, among their main causes, errors in perception (i.e., identification of an object, such as a car, a pedestrian or a cyclist) instead of errors in control (often caused by driver impairment, driver inexperience or speeding). Moreover, we focused on scenario groups with the highest fatality rates, strongly influenced by adverse weather conditions and poor visibility.

Even though 44% of the crashes in the ‘Control Loss’ group had adverse weather as the main factor, most of them had errors in control as their main cause. This may be attested by the fact that the average number of vehicles per crash is close to 1 and that, by definition, there are no external entities (e.g., animals, cyclists or pedestrians) involved in crashes in this group. A similar consideration may be made for the ‘Road Departure’ group.

Therefore, the most relevant groups, based on our criteria, are ‘Pedestrian’, ‘Pedalcyclist’, ‘Opposite Direction’ and ‘Crossing Paths’. The last two gain even more relevance given that they have the highest fatality rate for motorcyclists, according to a 2020 NHTSA report focused exclusively on crashes involving motorcycles [36].

From these four groups, we looked back at the detailed scenario statistics of the 2007 report [34] and collected the following data regarding the road configurations commonly present in these groups:

- **Pedestrian:** crashes happened mostly on urban roads

(65%), with crashes where the vehicle maneuvered happening mostly at intersections (81%) and without maneuver at non-junctions (55%);

- **Pedalcyclist:** evenly split between urban (54%) and rural (46%) roads, but happening more commonly at intersections (68%);
- **Opposite Direction:** mostly happening at rural roads (65%) and non-junctions (87%), with a significant percentage happening at non-level (34%) or curved roads (39%);
- **Crossing Paths:** even split between rural (53%) and urban (47%) roads, mostly happening at intersections (63%).

In light of this data, we selected five road configurations that cover all of the above cases and modelled them on the following CARLA maps [8]:

- 1) **Urban intersection** (straight and level) [Town03];
- 2) **Urban non-junction** (straight and level) [Town03];
- 3) **Rural intersection** (straight and level) [Town07];
- 4) **Rural straight non-junction** (level) [Town07];
- 5) **Rural curved non-junction** (non-level) [Town07].

We then drew inspiration from the single-vehicle Oxford RobotCar Dataset [37], wherein a specific route was traversed twice a week for a year, capturing diverse scenes along the same path. Building on this, we introduced variations to the road configurations to simulate how these locations change across days. The first variation was object density, with two levels: **sparse**, featuring a fixed number of vehicles and pedestrians per road configuration, and **dense**, which increases the number of pedestrians by 2.33 $\times$  and vehicles by 2.67 $\times$ , amplifying occlusion. The second variation was weather, with eleven weather/daytime conditions simulated in CARLA:

- **Clear weather** (Day and Night);
- **Light rain** (Day and Night);
- **Heavy rain** (Day and Night);
- **Fog** (Day and Night);
- **Foggy Heavy ran** (Day and Night);
- **Glare** (Day).

By combining 11 weather and 2 density levels across 5 road configurations, we created a total of 110 unique scenarios. This setup enables detailed comparisons between environmental factors, such as the impact of rain intensity across different locations or the effects of increased object

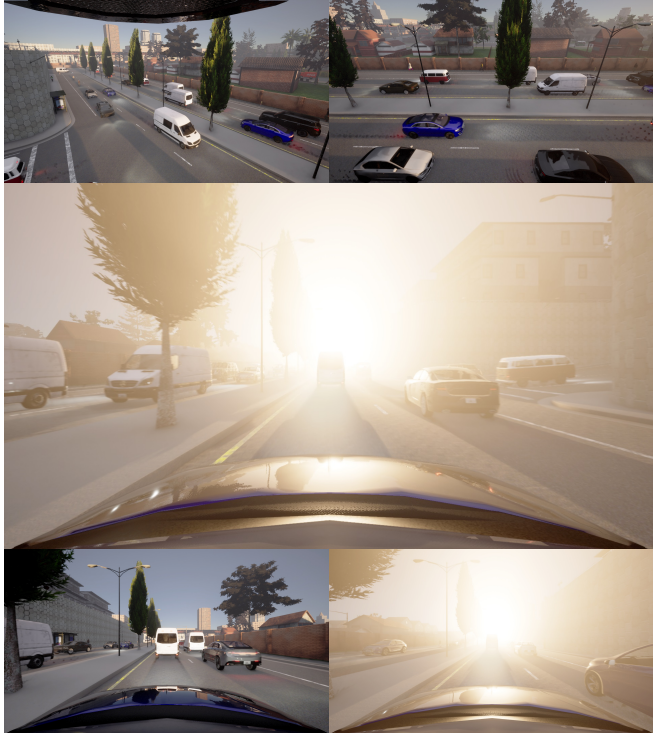


Fig. 2: Camera samples from the different viewpoints used in the Adver-City dataset. Scenario: glare day at urban non-junction. Top: RSUs, center: ego AV, bottom: connected AVs. Despite the ego’s front camera being heavily affected by glare, the RSUs remain unaffected, providing valuable information about the ego’s surroundings.

density at intersections. Despite stemming from only five road configurations, each scenario was simulated independently so that, for a given road configuration and density pairing, the agents’ behaviour varies slightly, resulting in a diverse set of simulations.

### B. Dataset Generation

The Adver-City dataset was generated in the CARLA simulator [8] with the OpenCDA [9] framework. Each scenario has data from five distinct viewpoints, as illustrated in Fig. 2: two RSUs, the ego vehicle, and two CAVs. Each viewpoint is equipped with the sensors listed in Table III.

Sensors	Details
4x RGB Camera	1920 × 1080, 100° horizontal FOV
4x Semantic Camera	1920 × 1080, 100° horizontal FOV
1x LiDAR	32 channels, 1.2M points/sec, 10Hz capture frequency, 200m range, $-25^\circ$ to $15^\circ$ vertical FOV*
GNSS & IMU	3e-6 std. dev. for latitude and longitude’s noise models, 0.05 std. dev. for altitude’s noise model

TABLE III: Sensor specifications for the AVs used in Adver-City scenarios. The RSUs are not equipped with GNSS & IMU but otherwise follow the same specification. \*RSUs positioned above ground have a  $-25^\circ$  to  $-1^\circ$  vertical FOV.

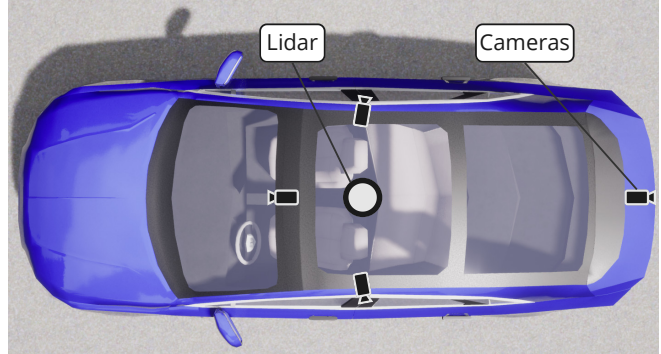


Fig. 3: Sensor positioning in CAVs. Camera positioning indicates both RGB and semantic segmentation cameras. Side-facing cameras are tilted backwards by 10° to reduce motion blur effects.

The sensor configuration was selected to balance detection performance with real-world feasibility. We used 1080p (1920 × 1080) cameras and 32-channel LiDARs while omitting depth cameras. The 1080p cameras offer more detailed imagery compared to lower resolution options and are relatively affordable and widely available. The 32-channel LiDARs offer less detail than 64-channel models but are also more accessible. Although depth cameras may provide unique information, they are rarely used in practice. None of the real-world datasets discussed in Section II use depth cameras; instead, they use LiDARs with fewer than 64 channels and cameras with a resolution of 1080p or higher.

The AVs’ sensors are positioned as illustrated in Fig. 3: the frontal camera is mounted on the windshield, the rear camera is located at the back of the trunk, side-facing cameras are placed at the top of the B-pillars (tilted backwards by 10° to reduce motion blur), and the LiDAR is positioned at the top of the vehicle. RSUs are either attached to tall structures (such as walls, towers, traffic light poles, or light posts) or positioned in high-visibility spots along the road. In non-junction scenarios, one CAV is positioned ahead of the ego vehicle, travelling in the same direction, while the other CAV is also ahead but travelling in the opposite direction. In intersection scenarios, CAVs approach the intersection from different roads compared to the ego vehicle.

Data is captured at 10Hz and adheres to an annotation schema compatible with OPV2V [16], with the main difference relating to the categories in our dataset. Unlike OPV2V, which only included cars and did not require category annotations for bounding boxes, our dataset has six categories: cars, pedestrians, vans, trucks, bicycles, and motorcycles.

### C. Dataset Statistics

Fig. 4 presents statistics for the Adver-City dataset. On average, scenarios last 21.9 seconds (219 frames at 10Hz) and contain 52 unique vehicles and 44 unique pedestrians. Overall, the dataset has 24,087 frames and 890,127 annotations pertaining to 11,418 vehicles and 4,840 pedestrians.

Fig. 4a and Fig. 4b highlight the diversity of environmental conditions on Adver-City, showing slight variations in the

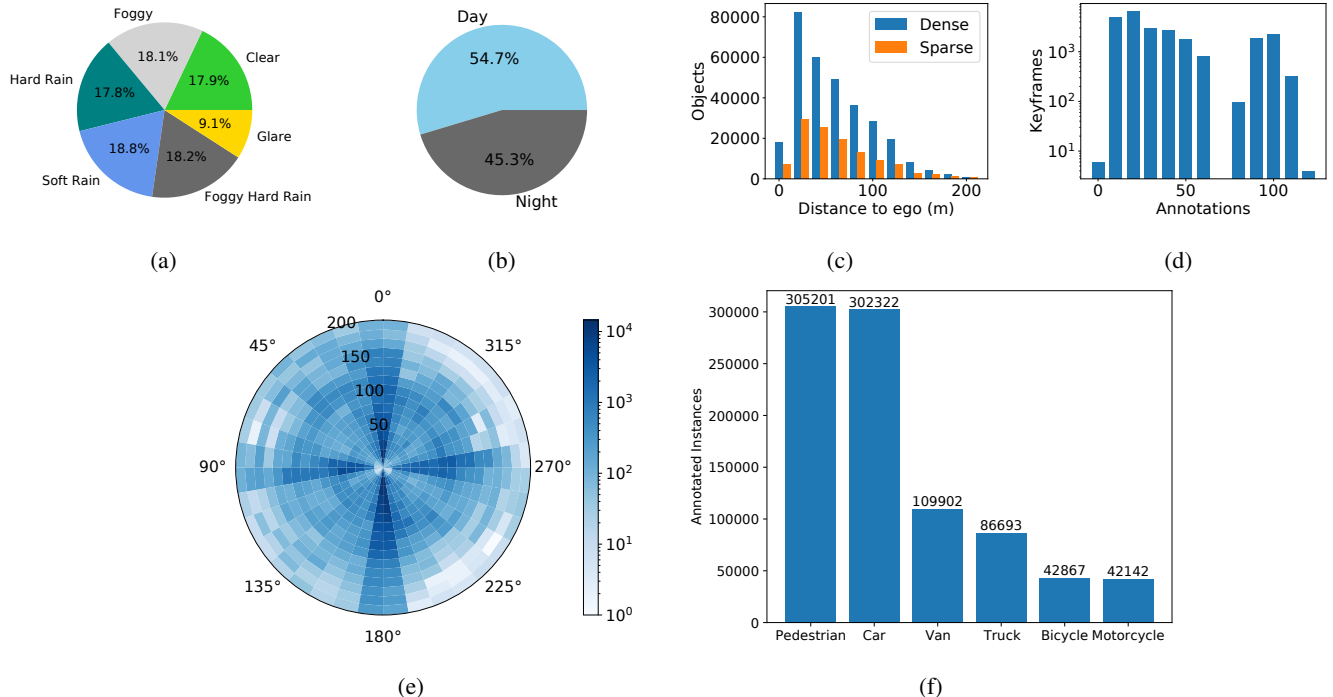


Fig. 4: Statistics for Adver-City. (a) Percentage of frames pertaining to each weather condition. (b) Percentage of frames per time of day. (c) Number of objects within line of sight of ego vehicle per distance to ego on dense and sparse scenarios. (d) Number of keyframes per annotation counts. (e) Polar density map in log scale for objects within line of sight of ego vehicle. Distance (in meters) and angle are in relation to ego, with the scale shown to the right. (f) Number of annotated instances per object class. Objects that are simultaneously detected by multiple viewpoints are not counted multiple times.

percentage of frames for each weather condition. These differences result from running scenarios individually, leading to minor variations in agent behaviour and consequently in scenario length. Fig. 4c shows the impact of density settings, with dense scenarios having significantly more objects, especially near the ego vehicle, compared to sparse ones.

Fig. 4d and Fig. 4e showcase the diversity of frames in Adver-City. The first shows the balance between the number of annotations in the keyframes, ranging from just a few to over 120 bounding boxes. The second shows that objects are positioned at various angles and distances from the ego vehicle, with a concentration around axial angles due to road layout. Fig. 4f highlights that the Pedestrian category has the highest number of annotated instances, making Adver-City well-suited for detecting Vulnerable Road Users (VRUs).

#### IV. BENCHMARK

How can a collaborative 3D object detection model trained without adverse weather generalize to adverse weather conditions? To answer that question, we used models trained on OPV2V [16] (which has no adverse weather) to perform inference on Adver-City, having as a baseline the Culver City testing scenario from OPV2V.

We tested the trained baseline models provided by the authors of HEAL [23] on Culver City, selecting the best-performing one for each sensor modality. Since the models for camera-based detection were trained with depth data, they

were disregarded from our analysis as the removal of depth made the models unsuitable for detection (the top camera-based model achieved an AP@50 of 19.02). Both for LiDAR and LiDAR + Camera detection, CoBEVT [22] was the best model for Culver City and was then used for inference in the Adver-City scenarios presented in Table IV. PointPillars [38] was used as the backbone for LiDAR models, and Lift-Splat-Shoot [39], with EfficientNet [40] as the image encoder, was used for camera experiments. All Adver-City experiments were conducted across the five road configurations described in Section III-A.

Even though our dataset follows the OPV2V annotation schema, minor adjustments were required to ensure the OPV2V-trained model performed adequately on Adver-City. Since OPV2V includes only the ‘car’ category, the model was limited to detecting cars. Bounding boxes for dissimilar categories such as ‘pedestrian’, ‘bicycle’, and ‘motorcycle’, were removed for the benchmark. Also, data from RSUs was excluded since OPV2V does not support V2X collaboration.

The average performance drop between Adver-City and Culver City (31% for both modalities) was due to differences in sensor configurations, positioning, and scenario locations. Despite this, clear patterns emerged: LiDAR-based detection was less impacted by adverse weather (3.9% variation between weather conditions, on average) than LiDAR + Camera (7.2% variation). On the other hand, LiDAR-based detection was more affected by higher object density (10.6%

Dataset	Scenario	Lidar (AP@50)				Lidar + Camera (AP@50)			
		Day		Night		Day		Night	
		Sparse	Dense	Sparse	Dense	Sparse	Dense	Sparse	Dense
Adver-City	Clear Weather	53.22	44.49	54.19	44.95	46.70	41.53	42.76	39.50
	Soft Rain	52.50	43.73	53.80	42.32	42.30	40.45	39.42	34.78
	Heavy Rain	54.38	42.05	49.42	44.71	43.06	38.72	34.11	38.03
	Fog	52.98	43.24	52.81	40.04	38.68	36.68	37.55	34.11
	Foggy Heavy Rain	54.31	42.97	54.42	38.76	37.83	35.77	40.40	34.18
	Glare	53.71	42.29	-	-	42.43	38.55	-	-
OPV2V [16]	Culver City	79.52		-		70.27		-	

TABLE IV: Benchmark results from 3D object detection models trained on OPV2V and tested with unseen data. All experiments used CoBEVT [22] models provided by the authors of HEAL [23]. PointPillars [38] was used as the backbone for Lidar, while Lift-Splat-Shoot [39] was used for camera with EfficientNet [40] as the image encoder. While Lidar experiments were more influenced by object density, Lidar + Camera experiments were more influenced by adverse weather conditions.

Scenario	Camera (mAP50)				Baseline (Day)	
	Day		Night			
	S	D	S	D		
Soft Rain	46.7	44.4	33.9	35.1	57.1 [43]	
Heavy Rain	42.1	41.8	21.5	27.7	46.0 [43]	
Fog	48.6	41.4	42.1	34.2	53.6 [44]	
Foggy Heavy Rain	38.7	40.9	34.4	26.7	-	
Glare	38.7	38.9	-	-	-	

TABLE V: Benchmark results from 2D object detection performed with YOLOv8 [41] on Adver-City’s adverse weather scenarios. S: sparse, D: dense. While glare was the most challenging condition for daytime scenarios, heavy rain was the toughest for nighttime.

variation) than LiDAR + Camera (3.0% variation).

Despite CARLA’s limitations, performance noticeably dropped as weather conditions became more challenging, with a 19% decline for the LiDAR + Camera model on sparse day scenarios. Moreover, the results highlight the diversity of Adver-City’s scenarios, with a performance gap of nearly 29% for LiDAR-based detection and 27% for LiDAR + Camera between the highest- and lowest-scoring scenarios.

Since camera-based 3D object detection was not viable with HEAL’s models, we performed 2D object detection with YOLOv8 [41] trained on the COCO dataset [42] to assess the impact of adverse weather on camera-based detection. The detection was done using only the front-facing camera of the ego vehicle. As shown in Table V, the model performed slightly below the baseline YOLO models on similar weather conditions, with results being impacted by nighttime by almost 26%.

Standing out from the 3D object detection benchmarks, object density played a lesser role in 2D object detection, with the median result being very similar both for sparse (38.7) and dense (38.9) scenarios, which is caused by different annotation strategies between the two tasks. While occlusion may heavily impact 3D detection, it is less prevalent in 2D detection because a completely occluded object will not have a corresponding 2D bounding box.

Therefore, even when using 2D object detection techniques, it might be important to correlate different cameras – from the ego vehicle, the connected vehicles, and the RSUs – for improved detection. This is a new avenue of research that can be explored with Adver-City.

## V. CONCLUSIONS

We introduced Adver-City, the first open-source dataset for Collaborative Perception (CP) focused on adverse weather conditions. Its scenarios, based on real-world data on adverse weather and poor visibility conditions, provide a valuable testbed for experimentation. Additionally, its variations in scene density and weather offer unique challenges for models tackling CP in complex environments.

Our benchmarks showed that models trained without adverse weather scenes suffer a significant drop in performance when used for inference in these conditions. In the future, we hope to investigate how existing CP models trained on Adver-City perform across its diverse weather conditions, but also to improve upon their designs to address shortcomings that may arise from their usage under adverse weather.

As an open-source dataset, Adver-City’s open code can be easily extended to include additional weather conditions such as snow or dust, new road configurations, and maps that leverage weather and density variations. Sensor configurations can also be adjusted to generate new data or enhance the realism of CARLA’s sensors. We hope its open-source nature encourages users to share their work, extending the benefits of collaboration beyond the confines of perception algorithms.

## REFERENCES

- [1] R. Bishop, “60 Million Miles And Counting: Robotaxis Shift Into High Gear,” *Forbes*, 2024. Available at <https://www.forbes.com/sites/richardbishop1/2024/07/27/60-million-miles-and-counting-robotaxis-shift-into-high-gear/>.
- [2] K. E. Trenberth and Y. Zhang, “How often does it really rain?,” *Bulletin of the American Meteorological Society*, vol. 99, no. 2, pp. 289 – 298, 2018.
- [3] J. Andrey and S. Yagar, “A temporal analysis of rain-related crash risk,” *Accident Analysis & Prevention*, vol. 25, no. 4, pp. 465–472, 1993.

[4] Ozarkar, Shailesh, Gely, Sandra, and Zhou, Kai, "Physics-based simulation solutions for testing performance of sensors and perception algorithm under adverse weather conditions," *SAE International Journal of Connected and Automated Vehicles*, vol. 5, pp. 297–312, apr 2022.

[5] Y. Zhang, A. Carballo, H. Yang, and K. Takeda, "Perception and sensing for autonomous vehicles under adverse weather conditions: A survey," *ISPRS Journal of Photogrammetry and Remote Sensing*, vol. 196, pp. 146–177, 2 2023.

[6] Y. Han, H. Zhang, H. Li, Y. Jin, C. Lang, and Y. Li, "Collaborative perception in autonomous driving: Methods, datasets and challenges," *IEEE Intelligent Transportation Systems Magazine*, vol. 15, pp. 131–151, 1 2023.

[7] T. Wang, S. Kim, J. Wenxuan, E. Xie, C. Ge, J. Chen, Z. Li, and P. Luo, "DeepAccident: A Motion and Accident Prediction Benchmark for V2X Autonomous Driving," *Proceedings of the AAAI Conference on Artificial Intelligence*, vol. 38, pp. 5599–5606, Mar. 2024.

[8] A. Dosovitskiy, G. Ros, F. Codevilla, A. Lopez, and V. Koltun, "CARLA: An open urban driving simulator," in *Proceedings of the 1st Annual Conference on Robot Learning*, pp. 1–16, 2017.

[9] R. Xu, Y. Guo, X. Han, X. Xia, H. Xiang, and J. Ma, "OpenCDA: an open cooperative driving automation framework integrated with co-simulation," in *2021 IEEE International Intelligent Transportation Systems Conference (ITSC)*, pp. 1155–1162, IEEE, 2021.

[10] H. Yu, Y. Luo, M. Shu, Y. Huo, Z. Yang, Y. Shi, Z. Guo, H. Li, X. Hu, J. Yuan, and Z. Nie, "DAIR-V2X: A Large-Scale Dataset for Vehicle-Infrastructure Cooperative 3D Object Detection," in *2022 IEEE/CVF Conference on Computer Vision and Pattern Recognition (CVPR)*, pp. 21329–21338, 2022.

[11] R. Xu, X. Xia, J. Li, H. Li, S. Zhang, Z. Tu, Z. Meng, H. Xiang, X. Dong, R. Song, H. Yu, B. Zhou, and J. Ma, "V2V4Real: A Real-World Large-Scale Dataset for Vehicle-to-Vehicle Cooperative Perception," in *2023 IEEE/CVF Conference on Computer Vision and Pattern Recognition (CVPR)*, pp. 13712–13722, 2023.

[12] W. Zimmer, G. A. Wardana, S. Sritharan, X. Zhou, R. Song, and A. C. Knoll, "TUMTraf V2X Cooperative Perception Dataset," in *Proceedings of the IEEE/CVF Conference on Computer Vision and Pattern Recognition (CVPR)*, pp. 22668–22677, June 2024.

[13] S. Manivasagam, S. Wang, K. Wong, W. Zeng, M. Sazanovich, S. Tan, B. Yang, W. Ma, and R. Urtasun, "Lidarsim: Realistic lidar simulation by leveraging the real world," in *2020 IEEE/CVF Conference on Computer Vision and Pattern Recognition (CVPR)*, (Los Alamitos, CA, USA), pp. 11164–11173, IEEE Computer Society, jun 2020.

[14] T.-H. Wang, S. Manivasagam, M. Liang, B. Yang, W. Zeng, and R. Urtasun, "V2VNet: Vehicle-to-Vehicle Communication for Joint Perception and Prediction," in *Computer Vision – ECCV 2020: 16th European Conference, Glasgow, UK, August 23–28, 2020, Proceedings, Part II*, (Berlin, Heidelberg), p. 605–621, Springer-Verlag, 2020.

[15] E. Arnold, S. Mozaffari, and M. Dianati, "Fast and robust registration of partially overlapping point clouds," *IEEE Robotics and Automation Letters*, vol. 7, no. 2, pp. 1502–1509, 2022.

[16] R. Xu, H. Xiang, X. Xia, X. Han, J. Li, and J. Ma, "OPV2V: An Open Benchmark Dataset and Fusion Pipeline for Perception with Vehicle-to-Vehicle Communication," *Proceedings - IEEE International Conference on Robotics and Automation*, pp. 2583–2589, 9 2021.

[17] Y. Li, D. Ma, Z. An, Z. Wang, Y. Zhong, S. Chen, and C. Feng, "V2X-Sim: Multi-Agent Collaborative Perception Dataset and Benchmark for Autonomous Driving," *IEEE Robotics and Automation Letters*, vol. 7, pp. 10914–10921, 2 2022.

[18] R. Mao, J. Guo, Y. Jia, Y. Sun, S. Zhou, and Z. Niu, "DOLPHINS: Dataset for Collaborative Perception enabled Harmonious and Interconnected Self-driving," *Lecture Notes in Computer Science (including subseries Lecture Notes in Artificial Intelligence and Lecture Notes in Bioinformatics)*, vol. 13845 LNCS, pp. 495–511, 7 2022.

[19] J. Gamerdinger, S. Teufel, P. Schulz, S. Amann, J.-P. Kirchner, and O. Bringmann, "SCOPE: A Synthetic Multi-Modal Dataset for Collective Perception Including Physical-Correct Weather Conditions," 2024. Available at <https://arxiv.org/abs/2408.03065>.

[20] Y. Lu, Q. Li, B. Liu, M. Dianati, C. Feng, S. Chen, and Y. Wang, "Robust collaborative 3d object detection in presence of pose errors," in *2023 IEEE International Conference on Robotics and Automation (ICRA)*, pp. 4812–4818, 2023.

[21] Y. Hu, S. Fang, Z. Lei, Y. Zhong, and S. Chen, "Where2comm: Communication-efficient collaborative perception via spatial confidence maps," in *Advances in Neural Information Processing Systems* (A. H. Oh, A. Agarwal, D. Belgrave, and K. Cho, eds.), 2022.

[22] R. Xu, Z. Tu, and H. X. W. S. B. Z. J. Ma, "CoBEVT: Cooperative Bird's Eye View Semantic Segmentation with Sparse Transformers," in *Conference on Robot Learning (CoRL)*, 2022.

[23] Y. Lu, Y. Hu, Y. Zhong, D. Wang, Y. Wang, and S. Chen, "An Extensible Framework for Open Heterogeneous Collaborative Perception," in *The Twelfth International Conference on Learning Representations*, 2024.

[24] Y. Hu, Y. Lu, R. Xu, W. Xie, S. Chen, and Y. Wang, "Collaboration helps camera overtake lidar in 3d detection," in *2023 IEEE/CVF Conference on Computer Vision and Pattern Recognition (CVPR)*, (Los Alamitos, CA, USA), pp. 9243–9252, IEEE Computer Society, jun 2023.

[25] Y. Hu, J. Peng, S. Liu, J. Ge, S. Liu, and S. Chen, "Communication-efficient collaborative perception via information filling with code-book," in *2024 IEEE / CVF Computer Vision and Pattern Recognition Conference (CVPR)*, 2024.

[26] Y. Li, J. Zhang, D. Ma, Y. Wang, and C. Feng, "Multi-robot scene completion: Towards task-agnostic collaborative perception," in *6th Annual Conference on Robot Learning*, 2022.

[27] Z. Lei, S. Ren, Y. Hu, W. Zhang, and S. Chen, "Latency-aware collaborative perception," in *Computer Vision – ECCV 2022: 17th European Conference, Tel Aviv, Israel, October 23–27, 2022, Proceedings, Part XXXII*, (Berlin, Heidelberg), p. 316–332, Springer-Verlag, 2022.

[28] Y. Li, S. Ren, P. Wu, S. Chen, C. Feng, and W. Zhang, "Learning distilled collaboration graph for multi-agent perception," in *Advances in Neural Information Processing Systems* (A. Beygelzimer, Y. Dauphin, P. Liang, and J. W. Vaughan, eds.), 2021.

[29] H. Caesar, V. Bankiti, A. H. Lang, S. Vora, V. E. Liong, Q. Xu, A. Krishnan, Y. Pan, G. Baldan, and O. Beijbom, "nuScenes: A multimodal dataset for autonomous driving," in *CVPR*, 2020.

[30] S. Singh, "Critical reasons for crashes investigated in the national motor vehicle crash causation survey," *Traffic Safety Facts - Crash Stats*, 3 2018.

[31] Q. Liu, X. Wang, S. Liu, C. Yu, and Y. Glaser, "Analysis of pre-crash scenarios and contributing factors for autonomous vehicle crashes at intersections," *Accident Analysis & Prevention*, vol. 195, p. 107383, 2 2024.

[32] Q. Liu, X. Wang, X. Wu, Y. Glaser, and L. He, "Crash comparison of autonomous and conventional vehicles using pre-crash scenario typology," *Accident Analysis & Prevention*, vol. 159, p. 106281, 9 2021.

[33] E. D. Swanson, F. Foderaro, M. Yanagisawa, W. G. Najm, P. Azeredo, and J. A. V. N. T. S. C. (U.S.), "Statistics of light-vehicle pre-crash scenarios based on 2011–2015 national crash data," 8 2019.

[34] W. G. Najm, J. D. Smith, M. Yanagisawa, and J. A. V. N. T. S. C. (U.S.), "Pre-crash scenario typology for crash avoidance research," 4 2007.

[35] T. Rothmeier, D. Wachtel, T. von Dem Bussche-Hünnefeld, and W. Huber, "I had a bad day: Challenges of object detection in bad visibility conditions," in *2023 IEEE Intelligent Vehicles Symposium (IV)*, pp. 1–6, 2023.

[36] E. D. Swanson, P. Azeredo, M. Yanagisawa, W. G. Najm, and J. A. V. N. T. S. C. (U.S.), "Pre-crash scenario characteristics of motorcycle crashes for crash avoidance research," 4 2020.

[37] W. Maddern, G. Pascoe, C. Linegar, and P. Newman, "1 Year, 1000km: The Oxford RobotCar Dataset," *The International Journal of Robotics Research (IJRR)*, vol. 36, no. 1, pp. 3–15, 2017.

[38] A. H. Lang, S. Vora, H. Caesar, L. Zhou, J. Yang, and O. Beijbom, "Pointpillars: Fast encoders for object detection from point clouds," in *2019 IEEE/CVF Conference on Computer Vision and Pattern Recognition (CVPR)*, pp. 12689–12697, 2019.

[39] J. Philion and S. Fidler, "Lift, splat, shoot: Encoding images from arbitrary camera rigs by implicitly unprojecting to 3d," in *Computer Vision – ECCV 2020* (A. Vedaldi, H. Bischof, T. Brox, and J.-M. Frahm, eds.), (Cham), pp. 194–210, Springer International Publishing, 2020.

[40] M. Tan and Q. Le, "EfficientNet: Rethinking model scaling for convolutional neural networks," in *Proceedings of the 36th International Conference on Machine Learning* (K. Chaudhuri and R. Salakhutdinov, eds.), vol. 97 of *Proceedings of Machine Learning Research*, pp. 6105–6114, PMLR, 09–15 Jun 2019.

[41] G. Jocher, A. Chaurasia, and J. Qiu, "Ultralytics YOLOv8," 2023. Available at <https://github.com/ultralytics/ultralytics>.

- [42] T.-Y. Lin, M. Maire, S. Belongie, L. Bourdev, R. Girshick, J. Hays, P. Perona, D. Ramanan, C. L. Zitnick, and P. Dollár, “Microsoft coco: Common objects in context,” 2015.
- [43] T. Kim, H. Jeon, and Y. Lim, “Challenges of yolo series for object detection in extremely heavy rain: Calra simulator based synthetic evaluation dataset,” 2023.
- [44] Z. Chu, “D-yolo a robust framework for object detection in adverse weather conditions,” 2024.